Electronic Supplementary Information (ESI)

The {Np_{38}} clusters: The missing link in the largest poly-oxo cluster series of tetravalent actinides

Nicolas P. Martin,[a] Christophe Volkringer,[a,b] Pascal Roussel,[a] Juliane März,[c]
Christoph Hennig,[c] Thierry Loiseau,*[a] and Atsushi Ikeda-Ohno*[c]

[a] *Unité de Catalyse et Chimie du Solide (UCCS), UMR, CNRS 8181, Université de Lille,*
École Nationale Supérieure de Chimie de Lille Centrale Lille,
Université Artois, 59000 Lille, France

[b] *Institut Universitaire de France, 1 rue Descartes, 75231 Paris Cedex 05, France*

[c] *Helmholtz-Zentrum Dresden-Rossendorf (HZDR), Institute of Resource Ecology,*
Bautzner Landstraße 400, 01328 Dresden, Germany

* E-mail: *thierry.loiseau@ensc-lille.fr* (T.L.) or *a.ikeda@hzdr.de* (A.I.-O.)

Table of Contents

1. Synthesis

Caution! Neptunium (^{237}Np) is a radioactive nuclide and, therefore, precautions with suitable equipment and facility for radiation protection are required for handling this radionuclide. All the experiments using ^{237}Np were carried out in a controlled laboratory at the Institute of Resource Ecology, Helmholtz-Zentrum Dresden-Rossendorf, Germany.

1-1. $NpCl_4$

The starting compound of $NpCl_4$ was prepared from NpO_2 according to the synthetic procedure to prepare UCl_4[1] with slight modification. NpO_2 was first dissolved in concentrated nitric acid (HNO_3) with gentle heating on a magnetic stirrer to convert into $NpO_2(NO_3)_2 \cdot nH_2O$ with dark-red colour. The resultant Np(VI)-nitrate compound was then transferred in hexachloropropene (C_3Cl_6) and heated with vigorous stirring under an inert atmosphere at ~470 K for 24 hours. This heating process in hexachloropropene leads to the reduction of Np(VI) to –(IV) and the chlorination simultaneously, resulting in the production of $NpCl_4$ as brownish precipitate. The resultant precipitate was then decanted to separate from the solvent, washed the precipitate with dichloromethane (dried and stored over $MgCl_2$) three times, and dried under an inert atmosphere. All the chemicals (except NpO_2) used in this study were analytical grade or higher, and used without further purification.

1-2. $Np_{38}O_{56}Cl_{18}(bz)_{24}(THF)_8 \cdot n$THF (**1**)

A mixture of 10 mg of $NpCl_4$ (0.026 mmol), 120 mg of benzoic acid (0.98 mmol), 0.5 mL of THF (6.16 mmol) and 2-20 μL of deionised water (1.11-11.1 mmol) was placed in a 2 mL glass vial and the vial was closed with a Teflon lid in an inert glove box filled with N_2 gas. The sample vial was then transferred into an oven and heated statically at 130 °C for 24 hours. After this process, small purple/brown octahedral crystals (~50 μm) appeared on the surface of the vial, together with dark polycrystalline or amorphous products, which are presumably Np(IV) oxy/hydroxides (Fig. 1-left in the main text). The crystals were then transferred directly into mineral oil and appropriate crystals were further selected under a polarised microscope for SC-XRD measurements. The formation of the additional polycrystalline/amorphous phase was promoted when the amount of deionised water added in the sample mixture increased. The best quality of crystals was obtained when 12 μL of deionised water was added in the sample mixture. Owing to the formation of the additional polycrystalline/amorphous phase and the limited amount of Np in the sample mixture (10 mg-$NpCl_4$), it was difficult to estimate the reaction yield for the formation of compound **1**. For the same reason, additional characterisation on compound **1** (e.g., powder-XRD, IR/Raman, elemental analysis, mass spectrometry, etc.) was not possible.

1-3. $Np_{38}O_{56}Cl_{42}(ipa)_{20} \cdot m$ipa (**2**)

A mixture of 10 mg of $NpCl_4$ (0.026 mmol), 10 mg of benzoic acid (0.082 mmol) and 1 mL of isopropanol (ipa, 13.1 mmol) was placed in a 2 mL glass vial and the vial was closed with a Teflon lid in an inert glove box filled with N_2 gas. The sample vial was then transferred into an oven and heated statically at 100 °C. After 3 days of heating, purple/brown octahedral crystals with ~50 μm appeared (Fig. 1-right in the main text) on the surface of the vial. Crystals were then transferred directly into mineral oil with the mother solution and further selected under a polarised microscope for SC-XRD measurements. For the same reasons as compound **1**, the estimation of reaction yield for compound **2** and additional characterisations on the compound were not possible.

2. Crystal structure determination

Crystal structure of the obtained {Np_{38}} compounds **1** and **2** was determined by single-crystal X-ray diffraction (SC-XRD). Crystals of the compounds **1** and **2** were selected under a polarizing optical microscope and mounted on a MicroMount™ supplied by MiTeGen with mineral oil. The SC-XRD measurements were performed on a Bruker D8 VENTURE diffractometer with a PHOTON 100 CMOS detector at 100 K using micro-focused Mo Kα radiation (λ = 0.71073 Å). Several sets of narrow data frames (20 s·frame^{-1}) were collected at different values of θ for two initial values of ϕ and ω, respectively, using 0.3° increments of ϕ or ω. Data reduction was performed using *SAINT Plus* (version 7.53a).[2] The substantial redundancy in the data allowed a semi-empirical absorption correction (*SADABS*, version 2.10)[3] to be applied, on the basis of multiple measurements of equivalent reflections. The structure was solved by direct methods, developed by successive difference Fourier syntheses, and refined by full-matrix least squares on all F2 data using the JANA2006 software.[4] Hydrogen atoms of organic molecules (benzoate, tetrahydrofuran and isopropanol) were placed at calculated positions and allowed to ride on their parent atoms. The final refinements include anisotropic thermal parameters of all non-hydrogen atoms.

The SC-XRD data collected for compound **1** was not of ideal quality, inducing some issues on the residual electron densities. This particularly results in relatively high electron densities remaining around the heaviest atoms (Np) and the atoms appearing on the surface of the {Np_{38}} clusters. For compound **1**, we observed disorder for benzoate groups. Consequently, these groups were treated as a rigid block and the positions and rotations of the entire blocks, instead of individual atomic positions, were refined with the help of a special function implemented on JANA2006. Additionally, the benzoate groups showing two distinct close positions for the aromatic ring (labelled with "B" for C and O atoms) were treated with a 50/50 occupancy. Another type of disorder was also observed between a terminal chlorine group (Cl4) and benzoate groups (labelled with "D" for C and O atoms). These two groups were also refined with a 50/50 occupancy with the help of a special function implemented on JANA2006.

In the structure refinement of compound **2**, the thermal parameters of some peripheral oxygen atoms have been refined isotropically, because only unreasonable values were obtained when they were refined anisotropically. Some of these oxygen atoms were fluctuated at two adjacent positions with isotropical thermal parameters. Some methyl groups in **2** were refined with disordered configurations, with occupying two close positions. The thermal parameters for the relevant carbon atoms were also refined isotropically. All the isopropanol molecules found in compound **2** exist as non-deprotonated neutral molecules, not as negatively charged isopropoxide molecules, although it is difficult to locate the position of the hydrogen atoms by SC-XRD.

The cif files provided with this publication contains several "Alert A" messages. The following is the explanation for the relevant "Alert A" messages.

<Compound **1**>
Isotropic non-H Atoms in Main Residue(s) 25 Report
This alert stems from the fact that most peripherical non H-atoms were refined isotopically due to the disordering of the molecules surrounding the cluster.

Check Calcd Resid. Dens. xA from Atom n
Check Negative Difference Density on Atom n
The relevant values reflect the disorder of different groups of the molecules around the cluster.

Check Calcd Positive Resid. Density on Npn
This relates to the potential issue of absorption correction adsorption. In case the absorption correction is not performed appropriately, it would affect the results mainly on the heaviest atoms (i.e. Np). This issue may originate from the fact that the amount of mineral oil, that was used to fix and maintain the crystal during the SC-XRD measurement, was too large, resulting in the distortion of the collected diffraction intensities.

<Compound **2**>
VERY LARGE Solvent Accessible VOID(S) in Structure
This message reflects the fact that no intercalated molecules were positioned amongst the {Np_{38}} cluster units. The position of the intercalated solvent molecules (i.e. isopropanol) could not be identified from the Fourier map analysis.

Check Calcd Resid. Dens. 0.12A From C2SAC
Check Calcd Resid. Dens. 0.15A From O1SA'C
These two messages originate from the disordering of the isopropanol molecules attached at the periphery of the {Np_{38}} cluster unit.

Table S1. Summary of crystal data and structure refinement for synthesised poly-oxo {Np_{38}} clusters obtained in THF (**1**) and in isopropanol (**2**)

	1	**2**
Formula	$C_{200}H_{184}Cl_{18}Np_{38}O_{112}$	$C_{60}H_{140}Cl_{42}Np_{38}O_{76}$
Formula weight	14025.5	12574.6
Temperature/K	100	100
Crystal type	brown octahedron	brown octahedron
Crystal size/mm	0.06 x 0.04 x 0.04	0.07 x 0.04 x 0.04
Crystal system	tetragonal	tetragonal
Space group	$I4/m$	$I4/m$
a /Å	21.9347(10)	19.5620(8)
b/Å	21.9347(10)	19.5620(8)
c/Å	29.8559(14)	29.3799(15)
α/°	90	90
β/°	90	90
Γ/°	90	90
Volume/$Å^3$	14364.6(11)	11242.9(11)
Z, $\rho_{calculated}$/$g.cm^{-3}$	2, 3.3427	2, 3.7145
μ/mm^{-1}	13.852	17.937
Θ range/°	2.19 – 26.43	2.33 – 26.37
Limiting indices	$-27 \leq h \leq 27$ $-37 \leq k \leq 37$ $-14 \leq l \leq 14$	$-24 \leq h \leq 20$ $-20 \leq k \leq 24$ $-25 \leq l \leq 36$
Collected reflections	165896	25716
Unique reflections	7828 [R(int) = 0.0617]	5873 [R(int) = 0.0709]
Parameters	193	202
Goodness-of-fit on F^2	3.63	1.23
Final R indices [$I>2\sigma(I)$]	$R1$ = 0.0697 $wR2$ = 0.0843	$R1$ = 0.0410 $wR2$ = 0.0774
R indices (all data)	$R1$ = 0.0985 $wR2$ = 0.0876	$R1$ = 0.1084 $wR2$ = 0.0910
Largest diff. peak and hole/e.$Å^{-3}$	9.88 and -3.38	3.55 and -5.51
CCDC deposition number	1840572	1840373

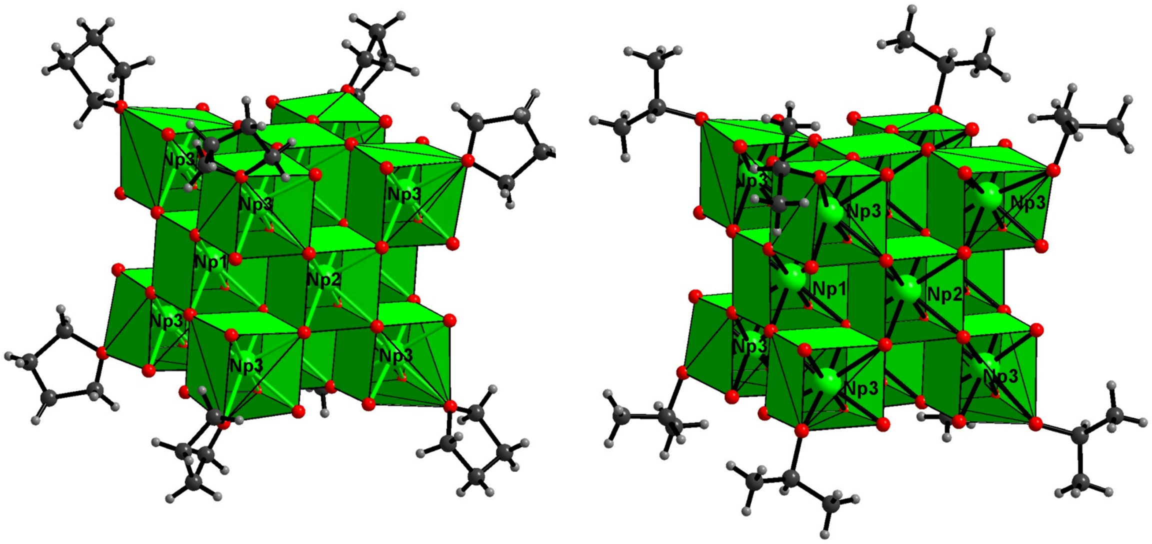

(a) (b)

Figure S1. Structure of the fluorite-based inner {Np_{14}} cores in the {Np_{38}} clusters **1** (a) and **2** (b). The coordination geometry around Np atoms (as Np^{4+}) is illustrated as light green polyhedra, whilst carbon (black), hydrogen (grey), and oxygen (red) atoms are shown as balls.

3. Total charge of the synthesised {Np_{38}} clusters

The SC-XRD analysis reveals the chemical formulae of [$Np_{38}O_{56}Cl_{18}(bz)_{24}(THF)_8$] and [$Np_{38}O_{56}Cl_{42}(ipa)_{20}$] for the {$Np_{38}$} clusters **1** and **2**, respectively. Assuming that all the Np atoms in the clusters are tetravalent (i.e. Np^{4+}), there is an excess negative charge of "-2" in both {Np_{38}} units. Such an excess negative charge of "-2" was also observed for the analogous {U_{38}} clusters synthesised in THF[5] and isopropanol.[6] The other analogous {An_{38}} clusters of Pu(IV) ({Pu_{38}}) also shows excess negative charges of "-2"[7] as well as "-14".[8] In the case of the {Pu_{38}} clusters, the excess negative charges of the {Pu_{38}} units are compensated with lithium cations (Li^+) intercalated in the crystal structures. However, in the case of the {U_{38}} clusters, no cations or cationic molecules are identified in the void space between the {U_{38}} units by SC-XRD, but only neutral molecules (THF or isopropanol) are identified. In this case, the excess negative charge of "-2" can be explained by the partial replacement of negative chlorides (Cl^-) with neutral water molecules (H_2O) on the surface of the clusters, or by the presence of μ_3-bridging hydroxo groups (OH^-) partially replacing the μ_3-oxo groups in the inner {U_{14}} core.[5, 6] As the crystal structures and obtained chemical formulae of the two {Np_{38}} clusters in **1** and **2** are well comparable to the analogous {U_{38}} clusters obtained in THF[5] and isopropanol,[6] respectively, the same explanation is applicable to interpret the excess negative charge of "-2" observed in the {Np_{38}} clusters. As a matter of fact, the analysis on the SC-XRD data for **2** indicates large anisotropic thermal parameters for the μ_3-oxo groups on the periphery of the inner {Np_{14}} core, potentially supporting the partial replacement the oxo groups with the hydroxo groups. In order to further investigate this possibility, the refinement by assuming the 2O/24OH for the splitting oxo atoms that show large anisotropic thermal parameters were attempted. That is, two close positions were assumed for the corresponding oxo groups with the help of a specific option on the software JANA, and the refinement was performed with an occupancy factor of the 'x/1-x' type. No H atoms (i.e. OH groups) are directly assumed on this refinement attempt. However, we can indirectly differentiate oxo- and hydroxo groups based on the calculated Np-O distances (i.e.

shorter- and longer Np-O distances for oxo- and hydroxo groups, respectively). The refinement converged, however, to a 50/50 occupancy without differentiating oxo- and hydroxo groups to obtain a neutral cluster. This suggests that the excess negative charge in the $\{Np_{38}\}$ clusters would be compensated by the combination of the partial replacement of Cl^- with H_2O and that of oxo groups with the hydroxo ones.

4. Structure comparison of tetranuclear complexes

Table S2. Summary of reported tetranuclear complexes of U(IV) and Th(IV) characterised in the solid state

ID	Compound	Tetranuclear core	Arrangement mode	An(IV) polyhedron	Bridging atoms	Reference
Tetra-U1	$U_4O_2(O_2CNEt_2)_4$	$U_4O_2(O_2CNEt_2)_4$	Plane	UO_8	μ_2- / μ_3-O	9
Tetra-U2	$[Cp(CH_3COO)_5U_2O]_2$	$[Cp(CH_3COO)_5U_2O]_2$	Plane	UO_8 + UO_6+pi	μ_2- / μ_3-O	10
Tetra-U3	$4[U(CF_3COO)_4(H_2O)_{0.5}]2(C_{18}H_{36}N_2O_6)$	$4[U(CF_3COO)_4(H_2O)_{0.5}]$	Plane	UO_8 + UO_9	μ_2- / μ_3-O	11
Tetra-U4	$[U(C_5H_5)(CH_3COO)_2]_4O_2$	$[U(C_5H_5)(CH_3COO)_2]_4O_2$	Plane	UO_6+pi	μ_2-O	12
Tetra-U5	$\{UCl[HB(3,5\text{-}Me_2Pz)_3]O\}_4$	$\{UCl[HB(3,5\text{-}Me_2Pz)_3]O\}_4$	Plane	UO_2+N_3+Cl	μ_2-O	13
Tetra-U6	$[U_4(L^*)_2(H_2L^*)_2(py)_2O][CF_3SO_3]_2$	$[U_4(L^*)_2(H_2L^*)_2(py)_2O]$	Boat conformation	UO_8+N + UO_6+N_2	μ_2- / μ_3-O	14
Tetra-U7	$[(Me_2Pz)_{10}U_4(kipl)_2]$	$[(Me_2Pz)_{10}U_4(kipl)_2]$	Plane	UN_8	μ_2- / μ_3-N	15
Tetra-U8	$[(Me_2Pz)_8U_4(kipl)_2]$	$[(Me_2Pz)_8U_4(kipl)_2]$	Boat conformation	UN_7 + UN_9	μ_2- / μ_3-N	15
Tetra-U9	$[(Me_2Pz)_{11}U_4(kipl)]$	$[(Me_2Pz)_{11}U_4(kipl)]$	Boat conformation	UN_7	μ_3-N	15
Tetra-U10	$(Hdma)[U_4O_2(bdc)_3(form)_7]$	$[U_4O_2(bdc)_3(form)_7]$	Plane	UO_8	μ_2- / μ_3-O	16
Tetra-Th1	$Th_4OCl_2I_6[\text{kappa2}(O,O')\text{-}\mu\text{-}O(CH_2)_2OCH_3]_6$	$Th_4OCl_2I_6[\text{kappa2}(O,O')\text{-}\mu\text{-}O(CH_2)_2OCH_3]_6$	Boat conformation	ThO_6+Cl+I	μ_4- / μ_2-O + μ_2-Cl	17

* H_4L = *N*,*N*'-bis(3-hydroxysalicylidene)-2,2-dimethyl-1,3-propanediamine

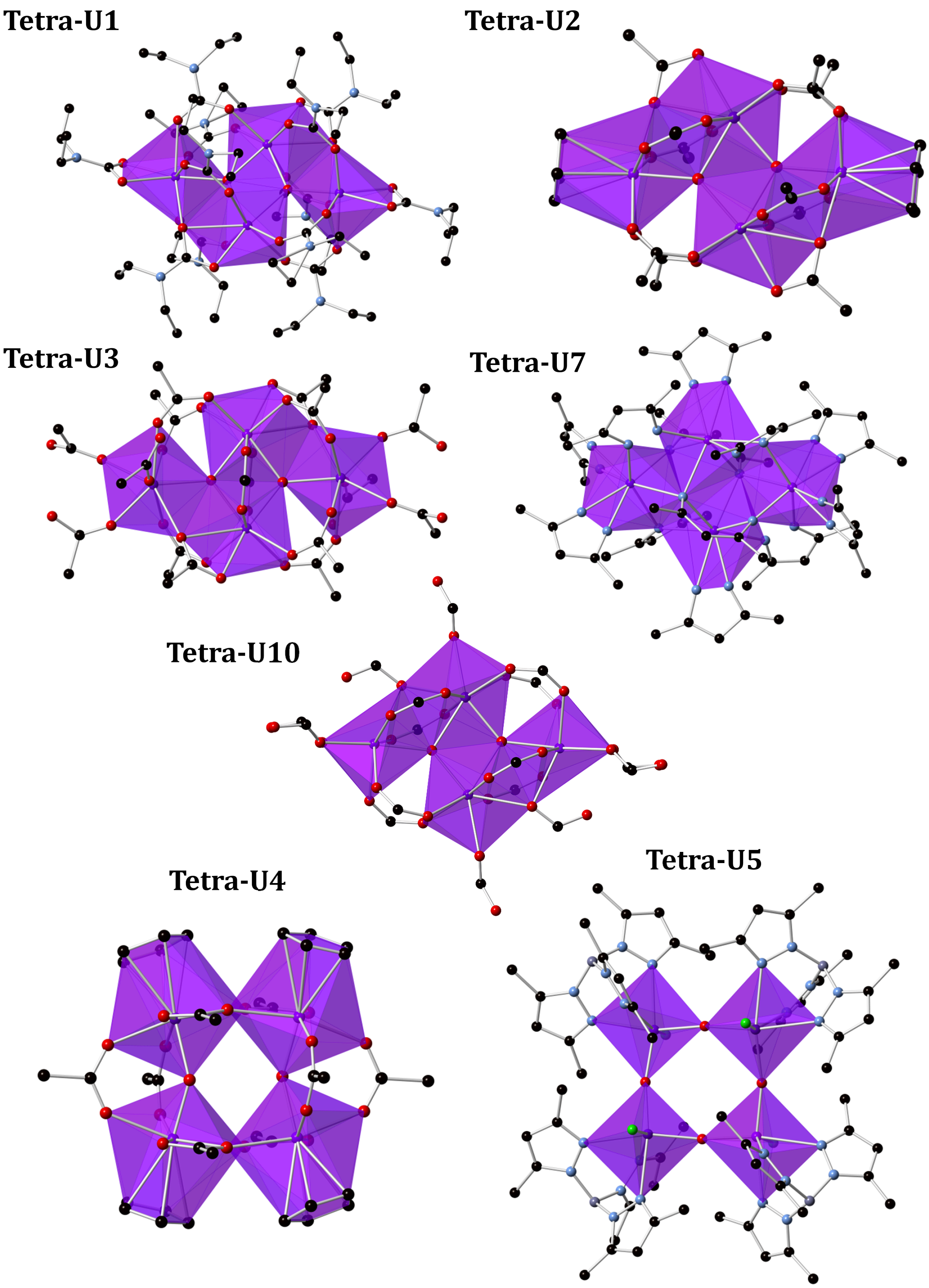

Tetra-U1

Tetra-U2

Tetra-U3

Tetra-U7

Tetra-U10

Tetra-U4

Tetra-U5

Figure S2. Molecular structures of planar tetranuclear U(IV) complexes listed in Table S2. The coordination geometry around U atoms (as U^{4+}) is illustrated as purple polyhedra, whilst carbon (black), chlorine (light green), nitrogen (blue) and oxygen (red) atoms are shown as balls. Hydrogen atoms are omitted for clarity.

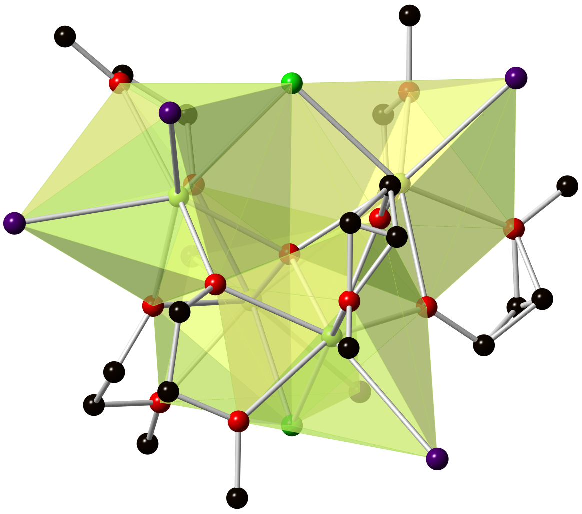

Figure S3. Molecular structure of the tetranuclear Th(IV) complex "Tetra-Th1" in Table S2. The coordination geometry around Th atoms (as Th^{4+}) is illustrated as pale-yellow polyhedra, whilst carbon (black), chlorine (light green), iodine (dark purple) and oxygen (red) atoms are shown as balls. Hydrogen atoms are omitted for clarity. The oxygen atom shown at the centre of the structure exhibits a unique μ_4-bridging coordination manner.

Table S3. Summary of U-U distances in the planar tetranuclear complexes of U(IV) listed in Table S2. The IDs in the table are identical to those in Table S2.

ID	Tetranuclear core	U-U distance / Å
Tetra-U1	$U_4O_2(O_2CNEt_2)_4$	3.702, 3.777, 4.021
Tetra-U2	$[Cp(CH_3COO)_5U_2O]_2$	3.697, 3.840, 4.015
Tetra-U3	$4[U(CF_3COO)_4(H_2O)_{0.5}]$	3.596, 3.943, 4.077
Tetra-U4	$[U(C_5H_5)(CH_3COO)_2]_4O_2$	3.934, 4.188
Tetra-U5	$\{UCl[HB(3{,}5\text{-}Me_2Pz)_3]O\}_4$	4.136, 4.181
Tetra-U7	$[(Me_2Pz)_{10}U_4(kipl)_2]$	3.721, 3.824, 3.912
Tetra-U10	$[U_4O_2(bdc)_3(form)_7]$	3.710, 3.887, 4.025

As summarised in Table S3 and illustrated in Fig. S4, the U-U distances found in the reported planar tetranuclear U(IV) complexes show a wide distribution from 3.596 to 4.181 Å, while the distance in bulk UO_2 is 3.866 Å.[18-21] In contrast, the Np-Np distances found in the $\{Np_4\}$ subunits in the $\{Np_{38}\}$ clusters **1** and **2** (average: 3.922 Å) are well comparable with those in the bulk NpO_2 (3.843 Å).[22,23] This indicates that the $\{Np_4\}$ subunits exhibit a closer structural conformity to the bulk NpO_2 than the discrete tetranuclear U(IV) complexes do to the bulk UO_2. This also applies to all the $\{An_4\}$ subunits in a series of the $\{An_{38}\}$ clusters, as the structural arrangement of the $\{An_4\}$ subunits is essentially the same regardless of the elemental difference.

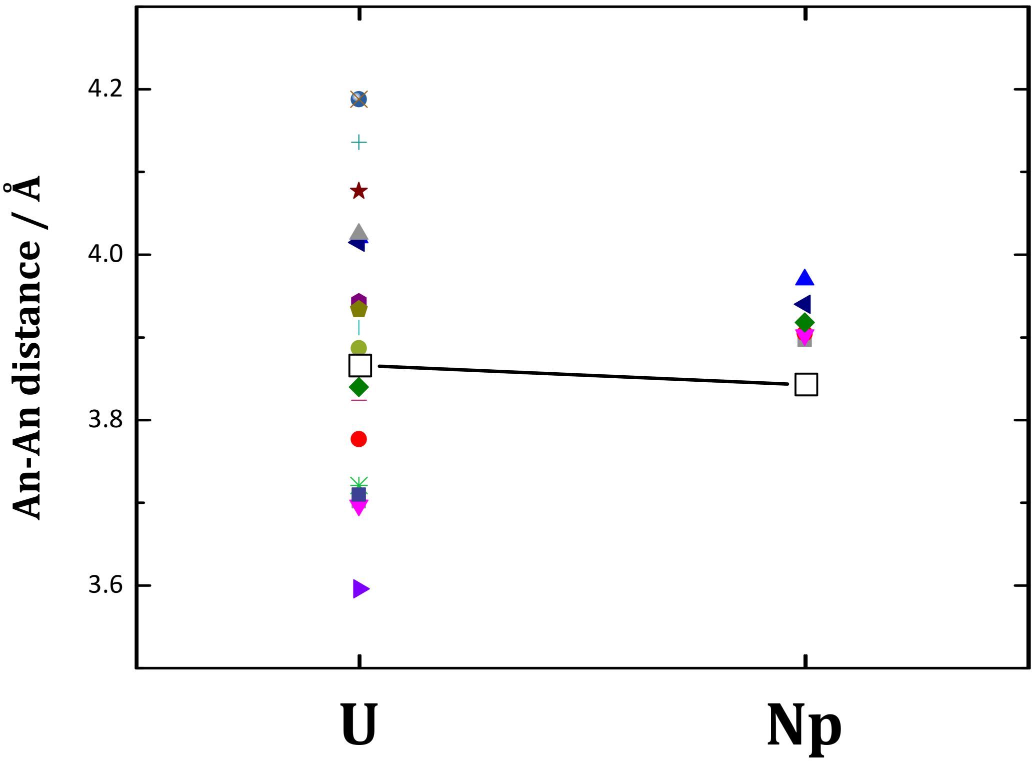

Figure S4. Distribution of An-An distances in bulk AnO_2 and planar tetranuclear An(IV) complexes (An = U and Np). White square boxes (□) linked with a black line correspond to the distances in the fluorite-based AnO_2 structure,[18-23] whilst the coloured plots represent the distances in the planar tetranuclear U(IV) complexes listed in Table S3 and those in the {Np_4} subunits in the {Np_{38}} clusters **1** and **2**.

References

1. D. Patel, A. J. Wooles, E. Hashem, H. Omorodion, R. J. Baker and S. T. Liddle, *New J. Chem.*, 2015, **39**, 7559-7562.
2. *SAINT Plus*, (2008) Bruker Analytical X-ray Systems, Madison, WI.
3. G. M. Sheldrick, *SADABS, Bruker-Siemens Area Detector Absorption and Other Correction*, (2008) Bruker Analytical X-ray Systems, Madison, WI.
4. V. Petříček, M. Dušek and L. Palatinus, *Z. Kristallogr. - Cryst. Mater.*, 2014, **229**, 345-352.
5. C. Falaise, C. Volkringer, J. F. Vigier, A. Beaurain, P. Roussel, P. Rabu and T. Loiseau, *J. Am. Chem. Soc.*, 2013, **135**, 15678-15681.
6. N. P. Martin, C. Volkringer, N. Henry, X. Trivelli, G. Stoclet, A. Ikeda-Ohno and T. Loiseau, *Chem. Sci.*, 2018, under revision.
7. R. E. Wilson, S. Skanthakumar and L. Soderholm, *Angew. Chem. Int. Ed.*, 2011, **50**, 11234-11237.
8. L. Soderholm, P. M. Almond, S. Skanthakumar, R. E. Wilson and P. C. Burns, *Angew. Chem. Int. Ed.*, 2008, **47**, 298-302.
9. F. Calderazzo, D. A. G., M. Pasquali and G. Perego, *Inorg. Chem.*, 1978, **17**, 474-479.
10. N. Brianese, U. Casellato, F. Ossola, M. Porchia, G. Rossetto and P. Zanella, *J. Organometall. Chem.*, 1989, **365**, 223-232.
11. P. Charpin, G. Folcher, M. Nierlich, M. Lance, D. Vigner, A. Navaza and C. De Rango, *Acta Crystallogr.*, 1990, **C46**, 1778-1781.
12. J. Rebizant, M. R. Spirlet and C. Apostolidis, *Acta Crystallogr.*, 1992, **C48**, 452-454.
13. A. Domingos, N. Marques, A. Pires De Matos, I. Santos and M. Silva, *Polyhedron*, 1992, **11**, 2021-2025.
14. L. Salmon, P. Thuéry and M. Ephritikhine, *Polyhedron*, 2006, **25**, 1537-1542.
15. J. D. Rinehart, S. A. Kozimor and J. R. Long, *Angew. Chem. Int. Ed.*, 2010, **49**, 2560-2564.
16. C. Falaise, C. Volkringer and T. Loiseau, *Cryst. Growth Design*, 2013, **13**, 3225-3231.
17. N. E. Travia, B. L. Scott and J. L. Kiplinger, *Chem. Eur. J.*, 2014, **20**, 16846-16852.
18. F. Hund, *Z. Anorg. Allg. Chem.*, 1964, **333**, 248-255.
19. M. J. Cooper, *Acta Crystallogr.*, 1982, **A38**, 264-269.
20. S. A. Barrett, A. J. Jacobson, B. C. Tofield and B. E. F. Fender, *Acta Crystallogr.*, 1982, **B38**, 2775-2781.
21. L. Desgranges, G. Baldinozzi, G. Rousseau, J. C. Niepce and G. Calvarin, *Inorg. Chem.*, 2009, **48**, 7585-7592.
22. W. H. Zacharlasen, *Acta Crystallogr.*, 1949, **2**, 388-390.
23. L. B. Asprey, F. H. Ellinger, S. Fried and W. H. Zacharlasen, *J. Am. Chem. Soc.*, 1955, **77**, 1707-1708.